Published in final edited form as:
Neuroimage. 2014 June ; 93 Pt 2: 165–175. doi:10.1016/j.neuroimage.2013.03.060.

Trends and Properties of Human Cerebral Cortex: Correlations with Cortical Myelin Content

Matthew F. Glasser[a], **Manu S. Goyal**[b], **Todd M. Preuss**[1,2,3], **Marcus E. Raichle**[a,b,c,d], and **David C. Van Essen**[a]

Manu S. Goyal: goyalm@mir.wustl.edu; Todd M. Preuss: tpreuss@emory.edu; Marcus E. Raichle: marc@npg.wustl.edu

[a]Department of Anatomy and Neurobiology, Washington University School of Medicine, 660 S. Euclid Avenue, St. Louis, MO 63110, USA

[b]Department of Radiology, Washington University School of Medicine, 660 S. Euclid Avenue, St. Louis, MO 63110, USA

[c]Department of Neurology, Washington University School of Medicine, 660 S. Euclid Avenue, St. Louis, MO 63110, USA

[d]Department of Biomedical Engineering, Washington University School of Medicine, 660 S. Euclid Avenue, St. Louis, MO 63110, USA

[1]Division of Neuropharmacology and Neurologic Diseases, Emory University School of Medicine, Atlanta, GA 30329, USA

[2]Center for Translational and Social Neuroscience, Yerkes National Primate Research Center, Emory University School of Medicine, Atlanta, GA 30329, USA

[3]Department of Pathology, Emory University School of Medicine, Atlanta, GA 30329, USA

Abstract

"*In vivo* Brodmann mapping" or non-invasive cortical parcellation using MRI, especially by measuring cortical myelination, has recently become a popular research topic, though myeloarchitectonic cortical parcellation in humans previously languished in favor of cytoarchitecture. We review recent *in vivo* myelin mapping studies and discuss some of the different methods for estimating myelin content. We discuss some ways in which myelin maps may improve surface registration and be useful for cross-modal and cross-species comparisons, including some preliminary cross-species results. Next, we consider neurobiological aspects of why some parts of cortex are more myelinated than others. Myelin content is inversely correlated with intracortical circuit complexity—in general, more myelin content means simpler and perhaps less dynamic intracortical circuits. Using existing PET data and functional network parcellations, we examine metabolic differences in the differently myelinated cortical functional networks.

Corresponding Author: David C. Van Essen, +1-314-362-7043 (tel), +1-314-747-3436 (fax), vanessen@.wustl.edu.
First Author: Matthew F. Glasser, +1-404-247-1694 (tel), +1-314-747-3436 (fax), glasserm@wusm.wustl.edu

Lightly myelinated cognitive association networks tend to have higher aerobic glycolysis than heavily myelinated early sensory-motor ones, perhaps reflecting greater ongoing dynamic anabolic cortical processes. This finding is consistent with the hypothesis that intracortical myelination may stabilize intracortical circuits and inhibit synaptic plasticity. Finally, we discuss the future of the *in vivo* myeloarchitectural field and cortical parcellation--"*in vivo* Brodmann mapping"--in general.

Keywords

Myelin Map; Cerebral Cortex; Aerobic Glycolysis; Cortical Area; PET; Cortical Parcellation

Introduction and Review

Oskar and Cécile Vogt, the foremost pioneers of the cortical parcellation enterprise, recognized in the early 20th century that myeloarchitecture is an important basis for parcellating cerebral cortex into cortical areas. They and some of their successors (most notably Adolf Hopf) produced detailed myeloarchitectonic parcellations of the human cerebral cortex. In humans, however, myeloarchitectonics was largely sidelined by a focus on cytoarchitecture, e.g. Brodmann's maps (see (Nieuwenhuys, 2012) for an excellent review of the history of human myelin-based cortical parcellation). Recently, cortical parcellation based on myelin content has remerged through the use of non-invasive MRI modalities (e.g. (Glasser and Van Essen, 2011), and reviewed below). Myeloarchitectural features have also begun to be measured non-invasively with high resolution MRI (e.g., < 0.5 mm voxel size), though this has largely been limited to area V1 (primary visual cortex) so far (e.g. (Geyer et al., 2011)). Accurate myeloarchitectural laminar profiles will require anatomically correct definition of the cortical layers (Waehnert et al., 2012) (Waehnert et al THIS ISSUE).

We focus here on surface-based analyses that respect the topology of the cortical sheet, but note that a few studies have examined myelin content or myeloarchitectural features in one or a few areas using a volumetric approach (some are reviewed in (Glasser and Van Essen, 2011)). Fischl et al (2004) reported the first non-invasive whole hemisphere group-average T1 maps of myelin content. These revealed the lightly myelinated anterior insular and cingulate cortices and the heavily myelinated sensori-motor and retrosplenial cortices (Fischl et al., 2004). The first detailed non-invasive surface-based study of a cortical area's myelin content was by Sigalovski et al (2006) who used 1/T1 maps (often called 'R1 maps') to identify the heavily myelinated auditory core, (primary auditory cortex) across individual subjects (Sigalovsky et al., 2006). Salat et al (2009) produced maps of grey matter T1w image intensity divided by subjacent white matter T1w intensity. Though they were interested in differences in T1w intensity throughout the adult lifespan, their maps have many of the variations that we now recognize as differences in cortical myelin content. In their whole brain group maps, they found all of the features present in Fischl et al (2004) plus increased T1w intensity in the visual cortex, and decreased T1w intensity in the temporal pole and dorsal/medial prefrontal cortex (Salat et al., 2009).

Bock et al. (2009, 2011) provided an important direct validation of non-invasive estimates of cortical myelin content in the marmoset monkey based on signal intensity variations in T1

maps and T1w images. By directly comparing T1 maps and T1w images to myelin stains in the same animals, they non-invasively identified myelin content features representing areas MT (middle temporal area), FEF (frontal eye fields), S1 (primary somatosensory cortex), M1 (primary motor cortex), A1 (primary auditory cortex), R (rostral auditory area), DM (dorsomedial area), V1, FST (fundus of superior temporal area), S2/PV (secondary somatosensory cortex, parietal ventral area), 12, and PPv (ventral posterior parietal cortex) using MRI and demonstrated correspondences with myelin stained sections (Bock et al., 2011; Bock et al., 2009). In another important validation study, Geyer et al (2011) showed that a post-mortem T1 map of human somatosensory cortex had an intensity border closely aligned with the myeloarchitectonically and cytoarchitectonically defined border between area 4 and area 3a, as seen in histological stains of the same piece of tissue.

These earlier validation papers provided valuable support for our interpretation that the T1w/T2w ratio is a reasonable estimate of relative myelin content across the cortical surface ("myelin maps") (Glasser and Van Essen, 2011). Using these myelin maps we identified dozens of features that represent putative cortical areas or areal borders. We showed both individual and group average data, but focused on the group average data for comparison and validation with previous cortical areal definitions. The first spatial derivative of the myelin map (i.e. the gradient magnitude) provided an observer-independent measure of the location and strength of myelin content transitions across the surface, which often represent putative areal borders. For example, the surface-based probabilistic maps (from cytoarchitectural histology) originally from Zilles and Amunts's groups (Fischl et al., 2008) had gradient defined areal borders in the same locations as the myelin maps between areas 6,4a+4p,3a,3b, and 1+2. We also demonstrated that myelin maps are informative not just for heavily myelinated areas but across the full spectrum of myelination, from very lightly myelinated anterior insula, cingulate, and temporal pole, to heavily myelinated area 4, V1, auditory core, and retrosplenial cortex. We compared myelin maps to many available histological cortical parcellation studies to identify myelin content features according to previous literature. In the cortex of the partieto-occipital sulcus, which has not previously been parcellated with histology in the human, we identified three areas with distinct myelin content: POS1, POS2, and POS3 (partieto-occipital sulcus areas 1–3). The myelin content feature corresponding to POS2 was later proposed to be the human homologue of macaque visual area V6A (Sereno et al., 2012). Finally, we discussed the correlations between myelin content and other properties of cortex, a topic we reconsider in an expanded context below.

Several subsequent studies have reported additional interesting results using in vivo mapping of cortical myelin content or myeloarchitecture. Sanchez-Panchuelo et al. (2011) compared 7T derived T2*w images with retinotopic fMRI activations in V1 and MT+ (middle temporal complex), demonstrating correspondence between the retinotopic borders of V1 and the stria of Gennari (also reported by (Bridge et al., 2005)) together with a colocalization of retinotopic MT+ with a T2*w hypointense band (Sánchez - Panchuelo et al., 2011). Cohen-Adad et al (2012) measured T2* across the entire cortical surface at 7T, identifying heavily myelinated visual, sensori-motor, auditory, and retrosplenial cortices as having lower T2* and lightly myelinated anterior cingulate and insula, medial and lateral prefrontal, and posterior cingulate cortices as having higher T2* (Cohen-Adad et al., 2012).

Expanding on this multi-modal approach, Sereno et al. 2012 carried out an informative comparison between in vivo myelin and retinotopic fMRI over a wide cortical expanse using 1/T1 maps. They focused on heavily myelinated regions of cortex that also showed retinotopic organization. Aside from confirming that sensory-motor cortex is heavily myelinated, they reported relatively heavily myelination of visual areas V1, V3A, MT, V6, V6A, V8/VO1, FST, and FEFs. They also found that heavily myelinated multi-modal areas LIP (lateral intraparietal area), VIP (ventral intraparietal area), and IFS (inferior frontal sulcus) had some retinotopic organization. Many of their proposed homology assignments between macaque invasively identified cortical areas and human non-invasive results seem plausible. However, their proposed homology of human and macaque VIP warrants further evaluation, e.g., using the same task paradigms in each species, as it is not easy to reconcile with our findings in myelin maps across humans, chimpanzees, and macaques (Glasser et al., 2012b). Other heavily myelinated regions illustrated but not discussed by Sereno et al. (2012) include 47m, PrCO (precentral opercular cortex), and pSTS (posterior superior temporal sulcus) as described by Glasser & Van Essen (2011). We are unable to tell whether their approach also reveals the lightly myelinated areas that we identified, because they chose to threshold their data.

Dick et al. (2012) extended the multi-modal approach to auditory cortex, examining tonotopically organized heavily myelinated auditory cortex with 1/T1 maps and tonotopic fMRI. They find that they can localize primary auditory cortical areas A1 and R using the combination of myelin content maps and tonotopic maps (Dick et al., 2012). Bock et al (2012) made an important methodological advance to in vivo myelin mapping, improving the T1w contrast for myelin in the MPRAGE sequence by increasing the delay between the MR inversion pulses. Though this increases scan duration, it improves CNR more effectively than the same amount of extra time spent averaging (Bock et al., 2012).

Commentary and Methodological Advances

Recently, we have implemented several methodological enhancements to the T1w/T2w myelin mapping technique. One important determinant of myelin map quality is the accuracy of the white matter surface and pial surface reconstructions used to delimit the cortical grey matter ribbon (Glasser and Van Essen, 2011). Standard 1mm isotropic voxels in humans are too coarse in resolution to accurately segment cortex in regions such as early visual cortex and primary somatosensory cortex, where cortical thickness is less than 2mm (or 2 voxels) as measured histologically by Von Economo and Koskinas (Triarhou, 2007). Additionally, gyral white matter blades in such regions may be even thinner, which further complicates cortical segmentation and surface generation. The Human Connectome Project (HCP) has addressed this problem by acquiring 0.7mm isotropic T1w and T2w images. In addition, the HCP processing pipelines (Glasser et al Submitted) take advantage of these higher resolution images with customizations introduced in the latest version of FreeSurfer (5.2) for final gradient-based surface placement (Glasser et al Submitted). Additionally, the T2w image is used to remove blood vessels and dura from the pial surface (they no longer need to be thresholded out of the T1w/T2w histogram as described in Glasser and Van Essen (2011)). The T2w image also enables grey matter specific intensity normalization to remove the effects of myelin content on pial surface generation (Glasser et al Submitted), improving

the robustness of the pial surface in very lightly myelinated cortical areas. Finally, the minor spatial distortion between T1w and T2w images caused by their differing readout bandwidth (van der Kouwe et al., 2008) is removed in the same way that distortion is removed from the phase encoding direction of EPI images, i.e., with a field map scaled according to the readout sample spacing (Glasser et al Submitted). The images are then registered with highly accurate cross-modal boundary-based registration techniques (Greve and Fischl, 2009). The result of these methodological improvements is much higher quality individual subject myelin maps, as illustrated by the unsmoothed myelin map in one individual (Figure 1), from the HCP Q1 public data release (http://www.humanconnectome.org/data/). Two kinds of myelin map artifacts from surface reconstruction errors, Type A errors of the white matter surface being placed too superficially and Type B errors of the pial surface being placed too deeply, are both greatly reduced by the above methodological improvements. Thus, the myelin map artifact correction steps described in Glasser and Van Essen (2011) are no longer needed. Additionally, cortical thickness measurements will be improved by these improvements in surface reconstruction.

The T1w/T2w myelin mapping method has been criticized because it does not measure a quantitative physical property of the tissue (as does a T1 map, which measures the longitudinal relaxation rate of protons within the tissue). Also, unlike receive field (B1−) biases, the T1w/T2w ratio cannot completely correct for transmit field (B1+) biases in intensity and contrast (Sereno et al., 2012), since they are only correlated between T1w and T2w, and not identical (Glasser and Van Essen, 2011). On the one hand, we strongly endorse the use of T1 maps by investigators who are able to acquire or access them and can also compensate for the B1+ effects that must also be corrected in T1 mapping to achieve accurate quantitative values (Sereno et al., 2012). Such T1 mapping, when correctly implemented, can indeed provide a more quantitative measure and be advantageous when making subtle quantitative comparisons across sites and scanners. T1 mapping methods (e.g. MP2RAGE, (Marques et al., 2010)) are also more appropriate at 7T, where T2w spin echo sequences face SAR limitations (though T1w and T2*w scans can be used (Martino et al., 2012)). On the other hand, it has not yet been established whether T1 maps, T1w/T2w ratio maps or other methods (like magnetization transfer maps) provide the best contrast to noise for discriminating neighboring cortical areas according to subtle relative differences in myelin content for the purpose of cortical parcellation. In our study (Glasser and Van Essen, 2011), we identified a larger number of myelin content features in T1w/T2w maps than have yet been identified by other investigators using other methods. Thus it would be interesting to directly compare T1w/T2w myelin maps to unthresholded group average myelin maps generated with different modalities after registration to a common surface atlas to determine whether there are differences in sensitivity to cortical areal boundaries across methods.

Regarding B1+ effects, T1w/T2w does enable reasonably good correction on scanners with good B1+ homogeneity. Figure 2 shows B1− receive field corrected (Siemens's prescan normalize) T1w and T2w images before and after correction using the sqrt(T1w X T2w) bias field correction approach, which is based on the same approximation as the T1w/T2w myelin mapping approach (Rilling et al., 2011). The corrected images are clearly more homogeneous. To enable interested investigators to model B1− and B1+ fields more precisely, the HCP is acquiring scans for mapping these intensity bias fields (head and body

coil images with the same sequence for B1− and AFI for B1+ (Yarnykh, 2007)). In post-processing, one can also explicitly remove very low spatial frequency differences (on the order of 20–30 mm FWHM) between the cortical hemispheres, or between biased individual and unbiased group average data, to greatly reduce any residual transmit field effects on the myelin maps (Glasser et al Submitted). When we compared two group average datasets acquired on different scanners, with different sequences, at different sites, we found qualitatively very similar overall results (Glasser and Van Essen, 2011). Finally, when the group average T1w/T2w myelin maps presented in Glasser and Van Essen et al (2011) are visually compared with T1 map-based myelin maps presented by Sereno et al (2012), there are no obvious qualitative differences in relative cortical areal myelin content across the surface. Thus, at 3T, T1w/T2w myelin mapping remains a particularly widely accessible method for mapping cortical areas in vivo in humans and non-human primates (Glasser et al., 2012b; Glasser et al., 2011b) based on relative differences in cortical myelin content.

Based on our experience with myelin mapping, we offer several practical suggestions for interested investigators. 1) Most previous in vivo studies have focused on heavily myelinated cortical areas, whereas myelin maps provide valuable information over the full spectrum of very lightly to very heavily myelinated cortex. To capitalize on this information, it is desirable to avoid thresholding the myelin maps and also to use a color scale that makes use of the full range of visible colors. Also, surface gradients provide an observer independent identification of the most likely locations of myelin content transitions. 2) With sufficient numbers of subjects (easily acquirable with T1w/T2w myelin mapping), we have found it unnecessary to smooth the resulting group average data. More recently, with high resolution T1w and T2w images, the individual data also do not need smoothing (Figure 1). Smoothing of myelin map data can obscure small but interesting features like area 3a, which is more lightly myelinated than surrounding cortex, but very narrow. 3) It is important to avoid the use of trilinear interpolation on images to be used for surface generation or myelin mapping, because this significantly increases the partial voluming between white matter, grey matter, and CSF (Glasser and Van Essen, 2011). Use of trilinear interpolation (or anything that results in significant unconstrained volumetric smoothing) reduces the accuracy of the surfaces generated and of the myelin maps. 4) Finally we offer some notes on acquisitions for T1w/T2w images: a) Both T1w and T2w images need to be high resolution (preferably smaller than 1mm isotropic). b) Fat saturation of the T2w image greatly reduces the usable contrast for myelin mapping (and T2w adjustment of the pial surface), likely due to reduction of magnetization transfer contrast (see below), and should thus be avoided. c) Conversely, fat saturation is highly desirable for T1w images, as it reduces the likelihood of surface reconstruction errors due either to fat shifted onto the brain or to bright fat in the marrow near the cortical surface. d) Our best results have been obtained using the gradient echo T1w MPRAGE and the variable flip angle spin echo T2w SPACE sequences.

Interestingly, the terms T1w and T2w are radiological terms that have little to do with the underlying physical contrast mechanisms present in the two images. In pure T2 maps there is little contrast between grey and white matter (Oros-Peusquens et al., 2008). Instead, the excellent grey/white contrast in the variable flip angle spin echo T2w SPACE sequence likely arises mostly from T1 and magnetization transfer (MT) effects (Thomas et al., 2004;

Weigel et al., 2010) (Turner, Robert: personal communication), which are both highly sensitive to myelin (Koenig, 1991; Rademacher et al., 1999). The gradient echo MPRAGE sequence has excellent grey/white contrast from T1 and T2* weighting (Van de Moortele et al., 2009), both of which also show contrast for myelin and also iron, which is colocalized with myelin in cortex (Fukunaga et al., 2010). Though the physical contrast mechanisms behind T1w/T2w myelin maps are complex, they produce excellent contrast to noise for variations in relative myelin content that can be used for a variety of purposes.

Future Uses of Myelin Content Mapping

In vivo MRI-based myelin maps provide an initial window into the architectonics of cerebral cortex in living brains that can also be studied with functional methods. It is highly desirable to compare myelin maps with other non-invasive imaging modalities, including resting state fMRI (Glasser et al., 2011a) and task fMRI (Glasser et al., 2012a). Intriguingly, many areal boundaries are colocalized between myelin maps and these fMRI methods, but there are also interesting complementarities. For example, all three modalities tend to show boundaries in the same location at the transition between one major functional region and another (e.g. between sensori-motor cortex and association cortex, or between visual cortex and association cortex). On the other hand, myelin maps currently show more areal definition within primary regions like somato-motor cortex, whereas the vast expanses of lightly myelinated association cortex are better defined using resting state or task fMRI.

Further evidence of the utility of myelin maps for understanding cortical organization comes from comparing them across humans, chimpanzees, and macaques (Glasser et al., 2012b; Glasser et al., 2011b). For example, Figure 3 reproduces a figure from Glasser et al 2012b showing myelin maps across humans, chimpanzees, and macaques. Similarities in the heavily myelinated areas (such as the early sensory and motor areas, MT+ complex, and retrosplenial cortex) and very lightly myelinated areas (such as the anterior cingulate, anterior insula, and temporal pole) can be easily recognized across the three species. It is also clear that cortex has undergone significant evolutionary change across species, with a vast expansion of the lightly myelinated (blue) regions (prefrontal cortex, inferior parietal cortex, and lateral temporal cortex) in humans in comparison to chimpanzees and macaques. This expansion is illustrated quantitatively in Figure 4, also reproduced from Glasser et al 2012b. The myelin content distribution peak in humans is on the lightly myelinated end of the spectrum whereas in macaques it is on the heavily myelinated end of the spectrum, with chimpanzees being intermediate, but closer to macaques than to humans. Further detailed discussion of these comparative myelin maps will be presented elsewhere.

Cortical areas are not constrained to lie in the same positions relative to cortical folds across individuals within a species (Amunts et al., 1999; Van Essen et al., 2012b), let alone across species separated by millions of years of evolution. Thus, myelin maps provide a tool for proposing putatively homologous regions and areas across species, both as an end in itself, and for other means. For example, using interspecies cortical surface registration to analyze the expansion of cortical regions during human evolution (Hill et al., 2010; Van Essen and Dierker, 2007) will likely benefit from landmarks delineated by myelin map transitions along with areal boundaries defined by other methods. Comparative tractography studies can

also use myelin maps to aid in drawing cortical seed and target ROIs that are more likely to be in homologous cortical regions (Rilling et al., 2011), rather than inferring homologous locations of ROIs based on sulcal geometry (Rilling et al., 2008).

Myelin maps will also be useful in comparisons between individuals within a species. Though surface-based nonlinear registration of the cerebral cortex is clearly superior to volume-based registration (Fischl et al., 2008; Frost and Goebel, 2012; Tucholka et al., 2012; Van Essen et al., 2012b), surface registration using shape features alone is unlikely to align those cortical areas with variable relationships to folding patterns across individuals (e.g. MT+/hOC5) (Glasser et al., 2012a; Van Essen et al., 2012b). Myelin content maps, which are closer than folding patterns to the underlying cortical architectonics and function, can improve cortical surface registration (Robinson et al., 2013). Such improvements in alignment across subjects will be invaluable for ongoing multi-modal non-invasive parcellation efforts and other group neuroimaging studies. Though there are many interesting uses for myelin maps, one that deserves further discussion here is the comparison between myelin maps and other trends and properties of human cerebral cortex.

Correlation of Myelin Maps with Other Cortical Architectural Properties

Myelin maps represented on standardized surface atlases enable comparisons with other data that have been brought onto the same atlas mesh (e.g. (Fischl et al., 2008; Glasser and Van Essen, 2011), and above). Mapping histological data onto this mesh can be difficult. Nonetheless, useful qualitative comparisons can be made with published histological data. For example, the 2D drawings of myelin content across the cortical surface by Adolf Hopf (Hopf, 1955, 1956; Hopf and Vitzthum, 1957) can be compared with in vivo myelin maps, revealing similar patterns of myelin content. The most basic observation is that primary sensory and motor areas tend to be the most heavily myelinated (Sanides, 1969) whereas association areas tend to be less heavily myelinated, though there are exceptions in both cases (Glasser and Van Essen, 2011).

Given the empirical fact that myelin density varies widely across the cortex, it is natural to wonder why some cortical areas are more heavily myelinated than others. Myelination surely evolved to speed axonal conduction (Hartline and Colman, 2007), and the amount of myelination increases for at least a portion of axons in white matter as brain size increases, maintaining a similar transmission latency across the larger brain (Wang et al., 2008). Axons in cat visual cortex have been shown to optimize their grey matter axonal arbor designs for both total “wire” length and timing precision (Budd et al., 2010), rather than just minimizing wire length. Also, long stretches of these axons lack synaptic boutons in grey matter and are presumed to be myelinated (Budd et al., 2010). Though myelin is important for conduction speed and timing, Braitenberg (1962) suggested an interesting additional possibility for why axons have stretches lacking synaptic boutons. He argued that the primary reason for myelination of axons in cortical grey matter is insulation to prevent formation of aberrant synapses and evolutionarily detrimental connections (Braitenberg, 1962). There is now a considerable amount of molecular evidence that factors associated with myelin inhibit both new axonal growth and synapse formation (Chen et al., 2000; Kapfhammer and Schwab, 1994; McGee and Strittmatter, 2003; McGee et al., 2005; McKerracher et al., 1994), which

may reduce the plasticity of heavily myelinated regions. In heavily myelinated primary visual cortex, the stria of Gennari is present even in congenitally blind subjects, suggesting that this myeloarchitectural feature is not very plastic, as it forms independently of visual experience and does not require visual experience to be maintained (Trampel et al., 2011).

Braitenberg (1962) also noted that most of the radial fibers in cortex are afferents specifically terminating in layers III and IV and efferents specifically originating from layers III and V. Tangential myelinated fibers are concentrated in the outer and inner bands of Baillarger and are mainly efferent axon collaterals running for some distance, 200–300um below the cell bodies of the originating pyramidal neurons (Braitenberg, 1962). Aside from these major myelinated fiber populations, other kinds of myelinated fibers are likely to contribute a smaller portion of the variation in overall cortical myelin content across six layered neocortical areas (Braitenberg, 1962). Though it varies from cortical area to cortical area, the myelin content profile from white surface to pial surface tends to decrease (from decreasing density of radial fibers) but has variable local increases as one crosses each tangential fiber population (Braitenberg, 1962). Thus, the in vivo myelin content measured in a cortical area will be mainly correlated with the density of radial and tangential fibers per unit cortical volume. These differences might be related to how much protection from synapse formation is required of the afferent and efferent connections or considerations of signal transmission speed and preciseness of timing in a cortical area.

Transitions in myeloarchitecture are closely correlated with transitions in cytoarchitecture (e.g. (Amunts et al., 2000; Geyer et al., 2011), reviewed (Nieuwenhuys, 2012)). An interesting but rarely cited study used cytoarchitectural profiles to predict myeloarchitecture in a computer simulation (Hellwig, 1993). The simulation used the cytoarchitectural profile plus two underlying assumptions: 1) That larger neurons contribute more to cortical myelin content than smaller ones and 2) That the density of axon collaterals at a given distance from the cell body can be modeled by a simple histogram (Paldino and Harth, 1977). Myelin content profiles predicted from cytoarchitecture alone in many cortical areas matched the major features in histological myelin stains of the same areas (Hellwig, 1993). These findings suggest that the laminar myeloarchitecture and cytoarchitecture are tightly linked.

Several other features of cortical architecture are correlated with myelin maps, including the density of neurons per unit cortical volume. Collins et al (2010) found that neuronal densities tend to be high in primary somatosensory and auditory cortex, and across many visual areas (Collins et al., 2010), which also have higher myelin content (Glasser and Van Essen, 2011). More lightly myelinated areas tended to have lower neuronal densities (Collins et al., 2010; Glasser and Van Essen, 2011), larger neuronal somata, and more complex intracortical circuitry, including larger dendritic field sizes, larger dendritic arbors, and more dendritic spines (Elston, 2000; Elston et al., 2001). This progression of increasing intracortical circuit complexity, spine density, and cell size is present in visual (Elston, 2002), somatosensory (Elston and Rockland, 2002), and motor cortex (Elston and Rockland, 2002) as one goes from early areas to late areas, whereas myelin content shows the opposite trend (Glasser and Van Essen, 2011). Additionally, humans tend to have more spines and complex dendritic arbors than macaques, particularly in prefrontal regions (Elston et al.,

2001; Elston et al., 2005), whereas human cortex is on average more lightly myelinated than macaque cortex (Glasser et al., 2012b; Glasser et al., 2011b).

Another important consideration involves regional differences in the relative thickness of cortical layers. The supragranular layers tend to be more lightly myelinated than the infragranular layers. Differences in the proportion of the cortical thickness devoted to supragranular vs infragranular layers may influence the myelin content measurement, which is an average across all the cortical layers in proportion to their volume. Some myelin content differences may simply reflect differences in the numbers of afferents and efferents per unit cortical volume (radial fiber densities) and differences in the number of efferent collaterals per unit cortical volume (tangential fiber densities). Heavily myelinated cortex is often thinner (Glasser and Van Essen, 2011), with larger numbers of neurons (Collins et al., 2010), which may have a larger number of inputs and outputs, but it also has smaller cells with simpler dendritic arbors (Elston, 2000; Elston et al., 2001), which take up less space. All these factors may increase the proportion of the available space filled with myelin relative non-myelin substances, leading to an increase in the relative myelin content in these cortical areas.

The main exceptions to the above trends are primary motor cortex and the other higher motor cortices. They have high myelin content (Glasser and Van Essen, 2011), but are thick (Triarhou, 2007), have low neuronal densities (Collins et al., 2010), and agranular cytoarchitecture (Triarhou, 2007). We speculated that the density of myelin content in cortical motor areas may relate to the strength of cortico-spinal projections and in particular to the proportion of axons travelling longer distances to lower regions of the spinal cord (Glasser and Van Essen, 2011). The Betz cells that project to the spinal cord are larger than typical pyramidal cells and tend to increase in size along the motor strip from the face representation to the foot representation (Rivara et al., 2003), corresponding to a parallel increase in myelin density (Glasser and Van Essen, 2011). The distribution of Betz cells declines only gradually at the border between area 4 and higher pre-motor areas (parts of area 6) (Geyer et al., 2000). Large pyramidal cells are also found in cingulate motor cortex (24d) (Braak, 1976). Myelin content in pre-motor and cingulate motor cortex is variable, tending to be higher closer to motor cortex and lower farther away from it (Glasser and Van Essen, 2011). Thus, variations in cortical spinal projections from Betz cells may impact myelin content in motor areas. How these myelin content variations outside primary motor cortex are related to somatotopy warrants further investigation using fMRI.

Other interesting correlations with myelin content involve developmental and evolutionary patterns. Paul Flechsig's map of the order of subcortical white matter myelination correlates with adult myelin maps (Glasser and Van Essen, 2011) (Sereno et al., 2012). Heavily myelinated areas, including primary sensory/motor areas and certain association areas (e.g. MT, 47m, IPS), tend to myelinate early, and lightly myelinated areas, largely association areas, tend to myelinate late (Glasser and Van Essen, 2011). Nonuniformities in postnatal cortical expansion, (Hill et al., 2010), also correlate with cortical myelin content. Heavily myelinated cortical areas tend to expand less after birth than lightly myelinated areas (Glasser and Van Essen, 2011). As noted previously (Hill et al., 2010), there is a strong correlation between areal expansion during development and areal expansion over the

course of evolution (Van Essen and Dierker, 2007). We extended this comparison to myelin maps, showing that lightly myelinated areas have expanded much more than heavily myelinated ones (Glasser and Van Essen, 2011). Future work will explicitly describe this relationship using myelin content homologies to constrain interspecies surface registration; however, it is clear from preliminary studies (e.g. Figures 3 and 4 above, (Glasser et al., 2012b; Glasser et al., 2011b)) that humans have undergone a large expansion of lightly myelinated association areas relative to chimpanzees or macaques. In summary, many architectural and other properties have been shown to correlate with myelin content. In the next section, we consider the relationship of myelin content to cortical metabolic properties.

Correlation of Myelin Maps with PET Metabolic Measures

To address how myelin content correlates with cortical metabolic parameters, we carried out a re-analysis of a the 33 subject resting state PET dataset from a previous study (Vaishnavi et al., 2010). Much of the processing was the same, except that we resampled the unsmoothed volumetric PET data (CMRGlu, CMRO2, CBF) into 1mm structural space and then onto each individual subject's cortical surface using a cortical ribbon-constrained approach similar to that presented in (Glasser and Van Essen, 2011). The cortical ribbon was defined in each PET subject using standard FreeSurfer 5.1 analysis on accompanying T1w MPRAGE scans. We corrected for partial volume effects when mapping the PET data onto the cortical surface with the assumption that the PET point spread function FWHM is ~6mm. This entailed constructing spatial partial volume regressors consisting of the effect of extra cerebral space (grey matter + white matter segmentation smoothed by 6mm), and the effect of the white matter (extracerebral space + grey matter segmentation smoothed by 6mm), both mapped onto the surface using the same ribbon-constrained approach. We modeled both partial volume effects separately because the magnitude of the effect of extracerebral space and white matter may not be the same on the surface grey matter PET data (Park et al., 2006). We then spatially regressed these quantities out of each PET map using a multiple regression. The PET maps were smoothed on the cortical surface by a geodesic distance of 11mm FWHM (the same as the 3D Cartesian distance used in Vaishnavi et al 2010). Finally, we performed the Glycolytic Index (GI) regression (Vaishnavi et al., 2010) between CMRGlu and CMRO2 on the smoothed surface data. The goal of this regression is to measure the proportion of glucose metabolism (measured with CMRGlu) that is in excess of what is required for oxidative phosphorylation, (measured by oxygen consumption, CMRO2). This fraction of glucose metabolism is known as aerobic glycolysis (for further details, see Vaishnavi et al (2010)). The surface-based regression yields a different numerical answer than that performed by Vaishnavi et al (2010) because we limited the regression to cortical grey matter, whereas their volumetric brain mask included cortical grey matter, subcortical grey matter, white matter, ventricles, and some extracerebral space. Performing the regression only on the cortical grey matter should maximally highlight differences between cortical regions.

Having the PET data mapped onto individual-subject cortical surfaces enabled us to use surface-based registration to average across subjects and compare the group average data directly to group average myelin maps (Glasser and Van Essen, 2011) on the same atlas surface mesh (Conte69 (Van Essen et al., 2012b)). Figure 5 shows myelin and GI maps on

medial and lateral views of both hemispheres; Supplementary Figure 1 shows maps of CMRGlu, CMRO2, and CBF. Higher aerobic glycolysis (very positive GI) occurs mainly in lightly myelinated association cortex of the frontal and parietal lobes. Very low aerobic glycolysis (very negative GI) occurs in very lightly myelinated cortex of the anterior insula, temporal pole, and anterior cingulate. In these regions, total glycolysis is much closer to the amount required for oxidative phosphorylation than in the regions with highly positive GI. Heavily myelinated primary sensory/motor cortex tends to have intermediate aerobic glycolysis (a GI of around or slightly above zero). Of the association cortices, prefrontal, medial parietal, posterior cingulate, posterior inferior parietal, and IPS cortices have the highest aerobic glycolysis (GI is very positive). Temporal cortex and anterior inferior parietal association cortices have lower aerobic glycolysis (GI slightly below zero), in contrast to the other lightly myelinated association areas.

To relate both cortical metabolic parameters and myelin to brain function, we used the functional network parcellations of Yeo et al 2011 and Power et al 2011, which are available on the same atlas surface mesh as our myelin and PET data. We calculated the mean myelin content value, GI value, CMRGlu value, CMRO2 value, and CBF value inside each network. The percentile relative to the full data range are reported in (Supplementary Tables 1 (Yeo et al., 2011) and 2 (Power et al., 2011)). Figure 6 shows the Yeo et al maps on the cortical surface with the mean value displayed in each functional network (see Supplementary Figure 2 for the corresponding Power et al 2011 map). The most heavily myelinated networks in both Yeo and Power et al (2011) are the sensori-motor, auditory, and visual networks (Yeo11: 1, 2, 3, 4, 5; Power11: 4, 5, 16, 24) along with the network that contains retrosplenial cortex and POS2 (Yeo11: 11; Power 22). The most lightly myelinated networks in both Yeo and Power et al (2011) are various association networks, including the default mode network, cingulo-opercular network, ventral attention network, and language network (Yeo11: 7, 8, 9, 10, 13, 16, 17; Power11: 3, 7, 14, 26). In between are other association networks like the dorsal attention network, the superior temporal gyrus network, and the fronto-parietal task control network (Yeo11: 6, 12, 14; Power11: 6, 9, 15). The functional networks with the highest aerobic glycolysis (GI) are a number of the association networks, including the fronto-parietal control network, the default mode network, the dorsal attention network, the ventral attention network, and the retrosplenial/POS2 network (Yeo11: 8, 11, 12, 13, 16; Power11: 3, 6, 7, 15, 22, 26). Lower aerobic glycolysis (GI) is found in the sensori-motor, auditory, and visual networks (Yeo11: 1, 2, 3, 4, 5, 6; Power11: 4, 5, 16, 24). Some other association networks also have lower aerobic glycolysis (GI), such as the superior temporal gyrus network and the cingulo-opercular network (Yeo11: 7, 14, 17; Power11: 9, 14). Though there are exceptions on both sides, primary sensory and motor networks tend to have higher myelin but lower aerobic glycolysis, whereas association networks tend to have lower myelin but higher aerobic glycolysis.

The generally higher aerobic glycolysis in lightly myelinated association cortex may be related to synaptic plasticity as mentioned above. Vaishnavi et al (2010) argued that increased synaptic plasticity might be one reason for elevated aerobic glycolysis. CMRGlu is elevated to twice adult levels during early childhood (2–10 years) (Chugani et al., 1987) when regions with high aerobic glycolysis also expand more than other cortical regions (Hill et al., 2010) and become myelinated according to Flechsig. Although GI has not been

measured during development, because there is not a corresponding increase in CMRO2 during this period of elevated CMRGlu (Takahashi et al., 1999), much of this increased glycolysis likely occurs beyond that required for oxidative metabolism. Thus, we would expect GI to be highly increased during early childhood. The increased glycolysis during early childhood may be used for anabolic processes in the developing human brain, an idea that would make sense given the developmental cortical expansion and subcortical myelination that are occurring at the same time. Given the inverse relationship in adults between cortical myelination and aerobic glycolysis, lightly myelinated areas may have greater synaptic plasticity than more heavily myelinated areas both during development, and in the adult brain. We speculate that the functions of the lightly myelinated cortical areas, largely higher order cognitive functions, may require more adaptable, dynamic, and plastic circuitry than heavily myelinated, less glycolytic cortical areas. These heavily myelinated regions, such as primary sensory or motor areas, may need to be more static and hardwired to perform their lower order sensory and motor functions. Thus, in may brain regions, cortical myelin content may be a surrogate for overall synaptic plasticity of functional networks and their constituent cortical areas.

It is important to note, however, that the association between myelination and GI is not a simple linear relationship. The very lightly myelinated cortical areas (black on the myelin maps), together with hippocampal and parahippocampal cortex have the lowest aerobic glycolysis in the cerebral cortex. Interestingly, the cortical areas with very light myelination are all the same type of cortex, namely proisocortex (Glasser and Van Essen, 2011). Presumably, some functional difference in these cortical areas explains both their light myelination and low aerobic glycolysis. Lightly myelinated regions in lateral temporal cortex and anterior inferior parietal cortex have a lower amount of aerobic glycolysis than other association areas. Interestingly, temporal cortex (TEa) tends to have less complex dendritic arbors and spine density than frontal cortex (Area 10) in the macaque (Elston et al., 2001). Also, temporal cortex is distinctly vulnerable during development relative to other cortical regions (Frye et al., 2010; Martinussen et al., 2005). Thus, the inverse relationship between myelin and GI is strongest for a subset of lightly myelinated association areas in prefrontal, medial parietal, and posterior and inferior parietal cortex.

Summary and Future Directions for in vivo Myeloarchitectonics

One of myelin’s functions in the cortical grey matter may be as an inhibitor of intra-cortical circuit plasticity. The more plastic regions are thicker, have more spines, more complex intracortical circuits, less myelin/volume, and generally use more glucose than expected under aerobic conditions. Early sensory areas may require less plasticity, and thereby require more myelination. Hierarchically higher association areas have less myelination, which might enable greater plasticity. Among macaques, chimpanzees, and humans, humans have more lightly myelinated cortex relative to heavily myelinated cortex, whereas macaques and chimpanzees have the opposite pattern. Human higher cognitive abilities such as language may require the significant expansion of more plastic lightly myelinated association cortex relative to the common set of heavily myelinated areas present across the three species. Interestingly, comparative genomics studies have suggested that relative to nonhuman primates, humans have modified the both expression and sequences of genes involved in

synapse formation and aerobic energy metabolism. Thus, the human brain may have a relatively higher energy expenditure than expected for its size and greater synaptic plasticity compared to the brains of nonhuman primates (Reviewed (Preuss, 2011)), perhaps because of the great expansion of the lightly myelinated and more plastic cortex.

To evaluate these hypotheses, experiments are needed that probe whether myelin has a causal or merely correlative relationship with synaptic plasticity. Beyond the overall association/primary dichotomy, there are additional details, including the very lightly myelinated regions having the lowest GI and a number of heavily myelinated regions having higher GI (e.g. within the IPS, in vicinity of POS2 and retrosplenial cortex, or in orbitofrontal cortex in 47m). Additionally the association cortex in the lateral temporal and anterior inferior parietal regions has a lower GI than other association regions.

Myelin content maps represent an initial step forward in *in vivo*, MRI-based architectonic analysis. Classical myeloarchitectonic studies have shown that some cortical areas can be discriminated by the laminar pattern of myelination (e.g., the prominence of inner and/or outer bands of Baillarger), not just by the overall degree of myelination (Hopf, 1955, 1956; Hopf and Vitzthum, 1957). Many additional cortical areas may be discriminable using high-resolution in vivo imaging of the laminar profiles of myelin content. Such analysis will benefit from higher field strength scanners (7T or higher), advanced motion correction techniques to reduce blurring, and improved algorithms (Waehnert et al., 2012) (Waehnert et al THIS ISSUE) to generate anatomically correct intermediate cortical surfaces that respect differences in laminar position caused by cortical folding in gyri and sulci (Bok, 1929). Before moving on to in vivo studies, these approaches will benefit from post-mortem imaging that offers some technical advantages and also allows direct comparisons with histology in the same brain.

The cortical parcellation problem inherent in the title of the special issue, “in vivo Brodmann mapping,” is indeed a difficult one. Cortical parcellations are most convincing when areal borders are present in multiple modalities in the same spatial locations (Zilles and Amunts, 2010). Myelin maps provide one of those modalities (Glasser and Van Essen, 2011). Resting state and task fMRI provide two others (Glasser et al., 2012a; Glasser et al., 2011a). However, subdivisions based on similarities in functional and anatomical connectivity often cut across well-defined architectonic areas (Van Essen and Glasser THIS ISSUE). While diffusion tractography has had significant success in reconstructing the major fiber pathways in humans (e.g. (Glasser and Rilling, 2008)) or across species (Rilling et al., 2011; Rilling et al., 2008), its use in parcellation of the cortical grey matter is still a work in progress. Fully surface-based tractography approaches will need to be cross-validated with other modalities, like myelin maps and fMRI, to see that they produce areal borders, rather than borders that are due to algorithmic biases or geometrical considerations like cortical folding or fascicle orientations in deep white matter (Van Essen et al., In Press). Cortical parcellation has been an ongoing enterprise for over a century (Nieuwenhuys, 2012), and even in the smaller, simpler, and much more studied macaque, a consensus parcellation has not yet been achieved (Van Essen et al., 2012a). Additionally, the hypothesis that all of cortex can be partitioned into areas has not yet been fully tested. Nevertheless, best guess predictions (Nieuwenhuys, 2012; Van Essen et al., 2012b) suggest

that there are 150–200 cortical areas in each human hemisphere. We therefore expect many exciting developments in the field of in vivo Brodmann mapping in the years to come.

Supplementary Material

Refer to Web version on PubMed Central for supplementary material.

Acknowledgments

We thank Russ Hornbeck and Lars Couture for providing the unresampled PET data in structural space. Yi Su and Avi Snyder provided helpful comments and discussion of the surface-based PET analysis strategy, including the partial volume correction methods. We thank Robert Turner for organizing the meeting in Leipzig that lead to this special topics issue, along with numerous helpful and enlightening discussions related to myelin mapping and in vivo Brodmann mapping in general. MFG was supported by an individual fellowship NIH F30 MH097312. Supported by NIH ROI MH-60974 and by the Human Connectome Project (1U54MH091657-01) from the 16 NIH Institutes and Centers that support the NIH Blueprint for Neuroscience Research. Support for PET data acquisition was provided by NS 06833. Chimpanzee and macaque data qcquisition was supported by NIH Grant P01AG026423.

References

Amunts K, Malikovic A, Mohlberg H, Schormann T, Zilles K. Brodmann's areas 17 and 18 brought into stereotaxic space—Where and how variable? Neuroimage. 2000; 11:66–84. [PubMed: 10686118]

Amunts K, Schleicher A, Bürgel U, Mohlberg H, Uylings H, Zilles K. Broca's region revisited: cytoarchitecture and intersubject variability. The Journal of comparative neurology. 1999; 412:319–341. [PubMed: 10441759]

Bock NA, Hashim E, Janik R, Konyer NB, Weiss M, Stanisz GJ, Turner R, Geyer S. Optimizing T_1-Weighted Imaging of Cortical Myelin Content at 3.0 Tesla. NeuroImage. 2012

Bock NA, Hashim E, Kocharyan A, Silva AC. Visualizing myeloarchitecture with magnetic resonance imaging in primates. Annals of the New York Academy of Sciences. 2011; 1225:E171–E181. [PubMed: 21599695]

Bock NA, Kocharyan A, Liu JV, Silva AC. Visualizing the entire cortical myelination pattern in marmosets with magnetic resonance imaging. Journal of neuroscience methods. 2009; 185:15. [PubMed: 19737577]

Bok ST. Der Einflu\ der in den Furchen und Windungen auftretenden Krümmungen der Gro\ hirnrinde auf die Rindenarchitektur. Zeitschrift für die gesamte Neurologie und Psychiatrie. 1929; 121:682–750.

Braak H. A primitive gigantopyramidal field buried in the depth of the cingulate sulcus of the human brain. Brain research. 1976; 109:219–233. [PubMed: 1276913]

Braitenberg V. A note on myeloarchitectonics. The Journal of comparative neurology. 1962; 118:141–156. [PubMed: 13872421]

Bridge H, Clare S, Jenkinson M, Jezzard P, Parker AJ, Matthews PM. Independent anatomical and functional measures of the V1/V2 boundary in human visual cortex. Journal of Vision. 2005:5.

Budd JML, Kovács K, Ferecskó AS, Buzás P, Eysel UT, Kisvárday ZF. Neocortical axon arbors trade-off material and conduction delay conservation. PLoS computational biology. 2010; 6:e1000711. [PubMed: 20300651]

Chen MS, Huber AB, van der Haar ME, Frank M, Schnell L, Spillmann AA, Christ F, Schwab ME. Nogo-A is a myelin-associated neurite outgrowth inhibitor and an antigen for monoclonal antibody IN-1. Nature. 2000; 403:434–439. [PubMed: 10667796]

Chugani HT, Phelps ME, Mazziotta JC. Positron emission tomography study of human brain functional development. Annals of neurology. 1987; 22:487–497. [PubMed: 3501693]

Cohen-Adad J, Polimeni J, Helmer K, Benner T, McNab J, Wald L, Rosen B, Mainero C. T_2* mapping and B_0 orientation-dependence at 7T reveal cyto-and myeloarchitecture organization of the human cortex. Neuroimage. 2012

Collins CE, Airey DC, Young NA, Leitch DB, Kaas JH. Neuron densities vary across and within cortical areas in primates. Proceedings of the National Academy of Sciences. 2010; 107:15927–15932.

Dick F, Tierney AT, Lutti A, Josephs O, Sereno MI, Weiskopf N. In Vivo Functional and Myeloarchitectonic Mapping of Human Primary Auditory Areas. The Journal of Neuroscience. 2012; 32:16095–16105. [PubMed: 23152594]

Elston GN. Pyramidal cells of the frontal lobe: all the more spinous to think with. J Neurosci. 2000; 20:1–4. [PubMed: 10627575]

Elston GN. Cortical heterogeneity: implications for visual processing and polysensory integration. Journal of neurocytology. 2002; 31:317–335. [PubMed: 12815250]

Elston GN, Benavides-Piccione R, DeFelipe J. The pyramidal cell in cognition: A comparative study in human and monkey. The Journal of Neuroscience. 2001

Elston GN, Benavides - Piccione R, Elston A, Zietsch B, DeFelipe J, Manger P, Casagrande V, Kaas JH. Specializations of the granular prefrontal cortex of primates: implications for cognitive processing. The Anatomical Record Part A: Discoveries in Molecular, Cellular, and Evolutionary Biology. 2005; 288:26–35.

Elston GN, Rockland KS. The pyramidal cell of the sensorimotor cortex of the macaque monkey: phenotypic variation. Cerebral Cortex. 2002; 12:1071–1078. [PubMed: 12217971]

Fischl B, Rajendran N, Busa E, Augustinack J, Hinds O, Yeo BTT, Mohlberg H, Amunts K, Zilles K. Cortical folding patterns and predicting cytoarchitecture. Cerebral Cortex. 2008; 18:1973–1980. [PubMed: 18079129]

Fischl B, Salat DH, van der Kouwe AJW, Makris N, Ségonne F, Quinn BT, Dale AM. Sequence-independent segmentation of magnetic resonance images. Neuroimage. 2004; 23:S69–S84. [PubMed: 15501102]

Frost MA, Goebel R. Measuring structural–functional correspondence: Spatial variability of specialised brain regions after macro-anatomical alignment. Neuroimage. 2012; 59:1369–1381. [PubMed: 21875671]

Frye RE, Malmberg B, Swank P, Smith K, Landry S. Preterm birth and maternal responsiveness during childhood are associated with brain morphology in adolescence. Journal of the International Neuropsychological Society. 2010; 16:784–794. [PubMed: 20609271]

Fukunaga M, Li TQ, van Gelderen P, de Zwart JA, Shmueli K, Yao B, Lee J, Maric D, Aronova MA, Zhang G. Layer-specific variation of iron content in cerebral cortex as a source of MRI contrast. Proceedings of the National Academy of Sciences. 2010; 107:3834–3839.

Geyer S, Matelli M, Luppino G, Zilles K. Functional neuroanatomy of the primate isocortical motor system. Anatomy and embryology. 2000; 202:443–474. [PubMed: 11131014]

Geyer S, Weiss M, Reimann K, Lohmann G, Turner R. Microstructural parcellation of the human cerebral cortex–from Brodmann's post-mortem map to in vivo mapping with high-field magnetic resonance imaging. Frontiers in human neuroscience. 2011:5. [PubMed: 21441977]

Glasser, MF.; Burgess, GC.; Xu, J.; He, Y.; Barch, DM.; Coalson, TS.; Fischl, B.; Harms, MP.; Jenkinson, M.; Patenaude, B.; Petersen, SE.; Schlaggar, BL.; Smith, S.; Woolrich, MW.; Yacoub, E.; Van Essen, DC. Surface Gradient Comparison of Myelin and fMRI: Architectonic and Functional Border Co-localization. Annual Meeting of the Organization for Human Brain Mapping; Beijing, China. 2012a.

Glasser, MF.; Laumann, T.; Coalson, T.; Cohen, A.; Snyder, A.; Schlaggar, B.; Petersen, S.; Van Essen, DC. Comparison of Surface Gradients Derived from Myelin Maps and Functional Connectivity Analysis. Annual Meeting of the Organization for Human Brain Mapping; Quebec City, Canada. 2011a.

Glasser, MF.; Preuss, TM.; Nair, G.; Rilling, JK.; Zhang, X.; Li, L.; Van Essen, DC. Improved Cortical Myelin Maps in Humans, Chimpanzees, and Macaques Allow Identification of Putative Areal Homologies. Society for Neuroscience; New Orleans, LA: 2012b.

Glasser, MF.; Preuss, TM.; Snyder, LH.; Nair, G.; Rilling, JK.; Zhang, X.; Li, L.; Van Essen, DC. Comparative Mapping of Cortical Myelin Content in Humans, Chimpanzees, and Macaques Using T1-weighted and T2-weighted MRI. Society for Neuroscience; Washington, DC: 2011b.

Glasser MF, Rilling JK. DTI tractography of the human brain's language pathways. Cerebral Cortex. 2008; 18:2471–2482. [PubMed: 18281301]

Glasser MF, Van Essen DC. Mapping human cortical areas in vivo based on myelin content as revealed by T1-and T2-weighted MRI. The Journal of Neuroscience. 2011; 31:11597–11616. [PubMed: 21832190]

Greve DN, Fischl B. Accurate and robust brain image alignment using boundary-based registration. Neuroimage. 2009; 48:63. [PubMed: 19573611]

Hartline D, Colman D. Rapid conduction and the evolution of giant axons and myelinated fibers. Current Biology. 2007; 17:R29–R35. [PubMed: 17208176]

Hellwig B. How the myelin picture of the human cerebral cortex can be computed from cytoarchitectural data. A bridge between von Economo and Vogt. Journal fur Hirnforschung. 1993; 34:387–387. [PubMed: 8270790]

Hill J, Inder T, Neil J, Dierker D, Harwell J, Van Essen D. Similar patterns of cortical expansion during human development and evolution. Proceedings of the National Academy of Sciences. 2010; 107:13135–13140.

Hopf A. Über die Verteilung myeloarchitektonischer Merkmale in der isokortikalen Schläfenlappenrinde beim Menschen. J Hirnforsch. 1955; 2:36–54.

Hopf A. Über die Verteilung myeloarchitektonischer Merkmale in der Stirnhirnrinde beim Menschen. J Hirnforsch. 1956; 2:311–333. [PubMed: 13376888]

Hopf A, Vitzthum HG. Über die Verteilung myeloarchitektonischer Merkmale in der Scheitellappenrinde beim Menschen. JOURNAL FÜR HIRNFORSCHUNG. 1957:3.

Kapfhammer J, Schwab ME. Inverse patterns of myelination and GAP - 43 expression in the adult CNS: Neurite growth inhibitors as regulators of neuronal plasticity? The Journal of comparative neurology. 1994; 340:194–206. [PubMed: 8201019]

Koenig SH. Cholesterol of myelin is the determinant of gray - white contrast in MRI of brain. Magnetic resonance in medicine. 1991; 20:285–291. [PubMed: 1775053]

Marques JP, Kober T, Krueger G, van der Zwaag W, Van de Moortele PF, Gruetter R. MP2RAGE, a self bias-field corrected sequence for improved segmentation and T_1-mapping at high field. Neuroimage. 2010; 49:1271–1281. [PubMed: 19819338]

Martino, FD.; Xu, J.; Glasser, M.; Essen, DV.; Moortele, P-Fvd; Goebel, R.; Formisano, E.; Ugurbil, K.; Yacoub, E. Enhanced Mylein-related contrast across the human brain at 7T using the ratio of high resolution T1 and T2* weighted images. ISMRM; Melbourne, Australia: 2012.

Martinussen M, Fischl B, Larsson H, Skranes J, Kulseng S, Vangberg T, Vik T, Brubakk AM, Haraldseth O, Dale A. Cerebral cortex thickness in 15-year-old adolescents with low birth weight measured by an automated MRI-based method. Brain. 2005; 128:2588–2596. [PubMed: 16123146]

McGee AW, Strittmatter SM. The Nogo-66 receptor: focusing myelin inhibition of axon regeneration. Trends in neurosciences. 2003; 26:193–198. [PubMed: 12689770]

McGee AW, Yang Y, Fischer QS, Daw NW, Strittmatter SM. Experience-driven plasticity of visual cortex limited by myelin and Nogo receptor. Science. 2005; 309:2222–2226. [PubMed: 16195464]

McKerracher L, David S, Jackson D, Kottis V, Dunn R, Braun P. Identification of myelin-associated glycoprotein as a major myelin-derived inhibitor of neurite growth. Neuron. 1994; 13:805–811. [PubMed: 7524558]

Nieuwenhuys R. The myeloarchitectonic studies on the human cerebral cortex of the Vogt–Vogt school, and their significance for the interpretation of functional neuroimaging data. Brain Structure and Function. 2012:1–50.

Oros-Peusquens A, Laurila M, Shah N. Magnetic field dependence of the distribution of NMR relaxation times in the living human brain. Magnetic Resonance Materials in Physics, Biology and Medicine. 2008; 21:131–147.

Paldino, A.; Harth, E. Computer Analysis of Neuronal Structures. New York: Plenum; 1977. A computerized study of Golgi-impregnated axons in rat visual cortex; p. 189-207.

Park HJ, Lee JD, Chun JW, Seok JH, Yun M, Oh MK, Kim JJ. Cortical surface-based analysis of 18F-FDG PET: measured metabolic abnormalities in schizophrenia are affected by cortical structural abnormalities. Neuroimage. 2006; 31:1434–1444. [PubMed: 16540349]

Power JD, Cohen AL, Nelson SM, Wig GS, Barnes KA, Church JA, Vogel AC, Laumann TO, Miezin FM, Schlaggar BL. Functional network organization of the human brain. Neuron. 2011; 72:665–678. [PubMed: 22099467]

Preuss TM. The human brain: rewired and running hot. Annals of the New York Academy of Sciences. 2011; 1225:E182–E191. [PubMed: 21599696]

Rademacher J, Engelbrecht V, Bürgel U, Freund HJ, Zilles K. Measuring in Vivo Myelination of Human White Matter Fiber Tracts with Magnetization Transfer MR. Neuroimage. 1999; 9:393–406. [PubMed: 10191168]

Rilling JK, Glasser MF, Jbabdi S, Andersson J, Preuss TM. Continuity, divergence, and the evolution of brain language pathways. Frontiers in evolutionary neuroscience. 2011:3. [PubMed: 21960970]

Rilling JK, Glasser MF, Preuss TM, Ma X, Zhao T, Hu X, Behrens TEJ. The evolution of the arcuate fasciculus revealed with comparative DTI. Nature neuroscience. 2008; 11:426–428.

Rivara CB, Sherwood CC, Bouras C, Hof PR. Stereologic characterization and spatial distribution patterns of Betz cells in the human primary motor cortex. The Anatomical Record Part A: Discoveries in Molecular, Cellular, and Evolutionary Biology. 2003; 270:137–151.

Robinson, EC.; Jbabdi, S.; Andersson, J.; Smith, S.; Glasser, MF.; Van Essen, DC.; Burgess, G.; Harms, M.; Jenkinson, M. Multimodal Surface Matching: a new surface registration approach that improves functional alignment. OHBM; Seattle, WA USA: 2013.

Salat D, Lee S, van der Kouwe A, Greve D, Fischl B, Rosas H. Age-associated alterations in cortical gray and white matter signal intensity and gray to white matter contrast. Neuroimage. 2009; 48:21–28. [PubMed: 19580876]

Sánchez -Panchuelo RM, Francis ST, Schluppeck D, Bowtell RW. Correspondence of human visual areas identified using functional and anatomical MRI in vivo at 7 T. Journal of Magnetic Resonance Imaging. 2011; 35:287–299. [PubMed: 21964755]

Sanides F. COMPARATIVE ARCHITECTONICS OF THE NEOCORTEX OF MAMMALS AND THEIR EVOLUTIONARY INTERPRETATION*. Annals of the New York Academy of Sciences. 1969; 167:404–423.

Sereno MI, Lutti A, Weiskopf N, Dick F. Mapping the Human Cortical Surface by Combining Quantitative T1 with Retinotopy. Cerebral Cortex. 2012

Sigalovsky IS, Fischl B, Melcher JR. Mapping an intrinsic MR property of gray matter in auditory cortex of living humans: a possible marker for primary cortex and hemispheric differences. Neuroimage. 2006; 32:1524. [PubMed: 16806989]

Takahashi T, Shirane R, Sato S, Yoshimoto T. Developmental changes of cerebral blood flow and oxygen metabolism in children. American journal of neuroradiology. 1999; 20:917–922. [PubMed: 10369366]

Thomas DL, De Vita E, Roberts S, Turner R, Yousry TA, Ordidge RJ. High - resolution fast spin echo imaging of the human brain at 4.7 T: Implementation and sequence characteristics. Magnetic resonance in medicine. 2004; 51:1254–1264. [PubMed: 15170847]

Trampel R, Ott DV, Turner R. Do the Congenitally Blind Have a Stria of Gennari? First Intracortical Insights In Vivo. Cerebral Cortex. 2011; 21:2075–2081. [PubMed: 21310782]

Triarhou LC. The Economo-Koskinas Atlas revisited: cytoarchitectonics and functional context. Stereotactic and Functional Neurosurgery. 2007; 85:195–203. [PubMed: 17534132]

Tucholka A, Fritsch V, Poline JB, Thirion B. An empirical comparison of surface-based and volume-based group studies in neuroimaging. NeuroImage. 2012

Vaishnavi SN, Vlassenko AG, Rundle MM, Snyder AZ, Mintun MA, Raichle ME. Regional aerobic glycolysis in the human brain. Proceedings of the National Academy of Sciences. 2010; 107:17757–17762.

Van de Moortele PF, Auerbach EJ, Olman C, Yacoub E, Uğurbil K, Moeller S. T1 weighted brain images at 7 Tesla unbiased for Proton Density, T2* contrast and RF coil receive B1 sensitivity with simultaneous vessel visualization. Neuroimage. 2009; 46:432. [PubMed: 19233292]

van der Kouwe AJW, Benner T, Salat DH, Fischl B. Brain morphometry with multiecho MPRAGE. Neuroimage. 2008; 40:559–569. [PubMed: 18242102]

Van Essen DC, Dierker DL. Surface-based and probabilistic atlases of primate cerebral cortex. Neuron. 2007; 56:209–225. [PubMed: 17964241]

Van Essen DC, Glasser MF, Dierker DL, Harwell J. Cortical parcellations of the Macaque monkey analyzed on surface-based atlases. Cerebral Cortex. 2012a; 22:2227–2240. [PubMed: 22052704]

Van Essen DC, Glasser MF, Dierker DL, Harwell J, Coalson T. Parcellations and hemispheric asymmetries of human cerebral cortex analyzed on surface-based atlases. Cerebral Cortex. 2012b; 22:2241–2262. [PubMed: 22047963]

Van Essen, DC.; Jbabdi, S.; Sotiropoulos, SN.; Chen, C.; Dikranian, K.; Coalson, T.; Harwell, J.; Behrens, TEJ.; Glasser, MF. Mapping Connections in Humans and Nonhuman Primates: Aspirations and Challenges for Diffusion Imaging. In: Behrens, TEJ.; Johansen-Berg, H., editors. Diffusion MRI. In Press

Waehnert, M.; Weiss, M.; Streicher, M.; Bazin, P.; Geyer, S.; Turner, R. Do cortical layers conform to the Laplace equation?. Annual Meeting of the Organization for Human Brain Mapping; Beijing, Beijing, China. 2012.

Wang SSH, Shultz JR, Burish MJ, Harrison KH, Hof PR, Towns LC, Wagers MW, Wyatt KD. Functional trade-offs in white matter axonal scaling. The Journal of Neuroscience. 2008; 28:4047–4056. [PubMed: 18400904]

Weigel M, Helms G, Hennig J. Investigation and modeling of magnetization transfer effects in two - dimensional multislice turbo spin echo sequences with low constant or variable flip angles at 3 T. Magnetic Resonance in Medicine. 2010; 63:230–234. [PubMed: 19859950]

Yarnykh VL. Actual flip - angle imaging in the pulsed steady state: A method for rapid three - dimensional mapping of the transmitted radiofrequency field. Magnetic resonance in Medicine. 2007; 57:192–200. [PubMed: 17191242]

Yeo BTT, Krienen FM, Sepulcre J, Sabuncu MR, Lashkari D, Hollinshead M, Roffman JL, Smoller JW, Zöllei L, Polimeni JR. The organization of the human cerebral cortex estimated by intrinsic functional connectivity. Journal of neurophysiology. 2011; 106:1125–1165. [PubMed: 21653723]

Zilles K, Amunts K. Centenary of Brodmann's map—conception and fate. Nature Reviews Neuroscience. 2010; 11:139–145.

Highlights

- Interest in *in vivo* myelin mapping using MRI is rapidly growing
- Many architectural properties of cerebral cortex are correlated with myelin content
- Cortical aerobic glycolysis is correlated with myelin content
- Cortical myelin may serve as an inhibitor of synaptic plasticity
- Multi-modal cortical parcellation will provide many new insights in the future

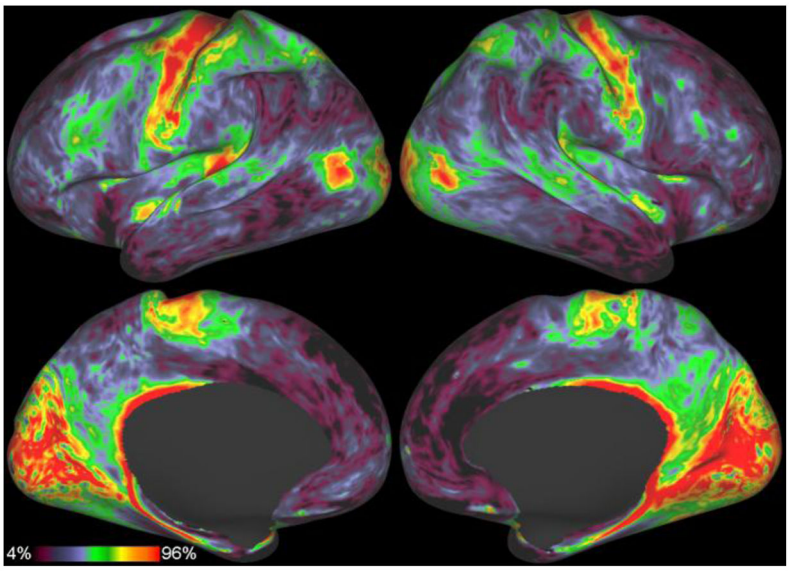

Figure 1.

Single subject unsmoothed myelin map from the 0.7mm isotropic publically released HCP data. Medial wall is masked in black. Color scale ranges from 4% (black) to 96% (red).

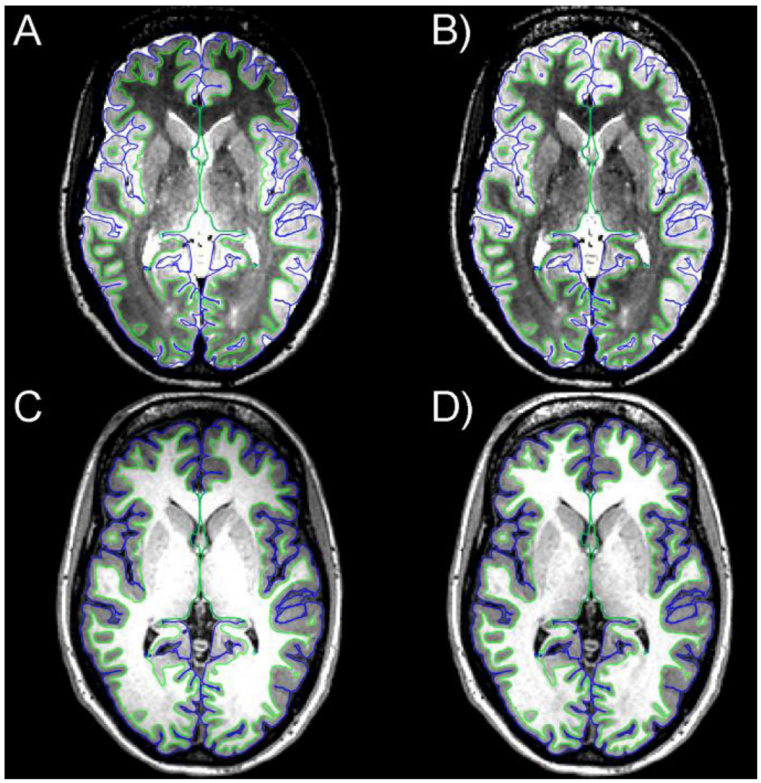

Figure 2.

Pre-scan normalized (i.e. Siemens scanner corrected for B1− receive field) T2w (A) and T1w (C) images. sqrt(T1w X T2w) bias field corrected T2w (B) and T1w (D) images. The corrected images are more homogeneous because the B1+ transmit field is correlated between the T1w and T2w images.

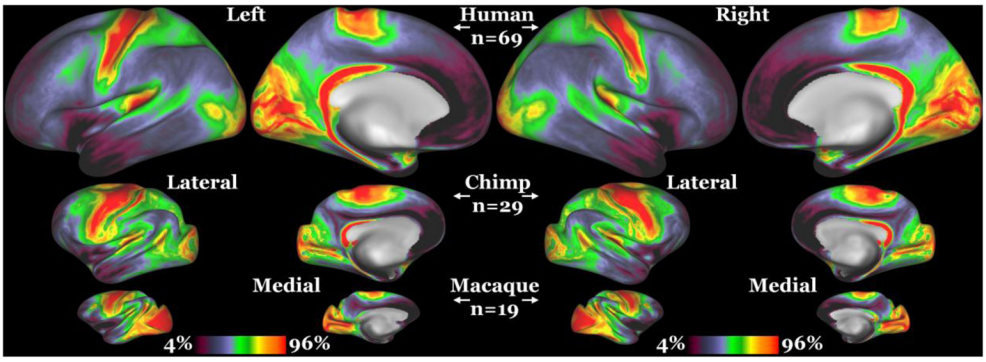

Figure 3.

Group average myelin maps from 69 humans, 29 chimpanzees, and 19 macaques scaled according to brain size. Many areal homologies are suggested by similarities in the maps across species, but differences are also apparent. More of the expansion in brain size has come from lightly myelinated (blue) areas vs from heavily myelinated (red/orange/yellow) or very lightly myelinated areas (black/purple). Adapted from Glasser, M.F., Preuss, T.M., Nair, G., Rilling, J.K., Zhang, X., Li, L., Van Essen, D.C., 2012b.

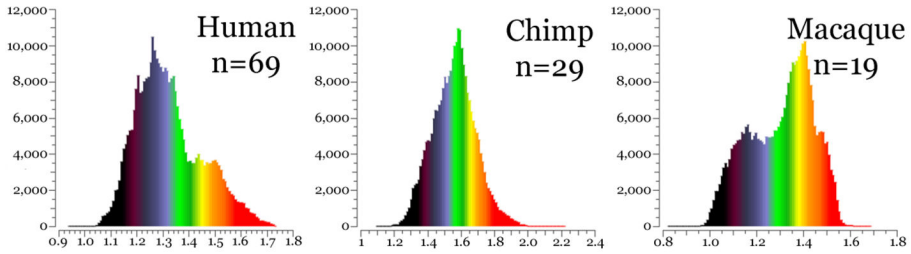

Figure 4.

Histograms of myelin map values across humans, chimpanzees, and macaques. The peak of the distribution is in the lightly myelinated areas in humans but in the heavily myelinated areas in macaques, with chimpanzees intermediate but closer to macaques than to humans. Adapted from Glasser, M.F., Preuss, T.M., Nair, G., Rilling, J.K., Zhang, X., Li, L., Van Essen, D.C., 2012b.

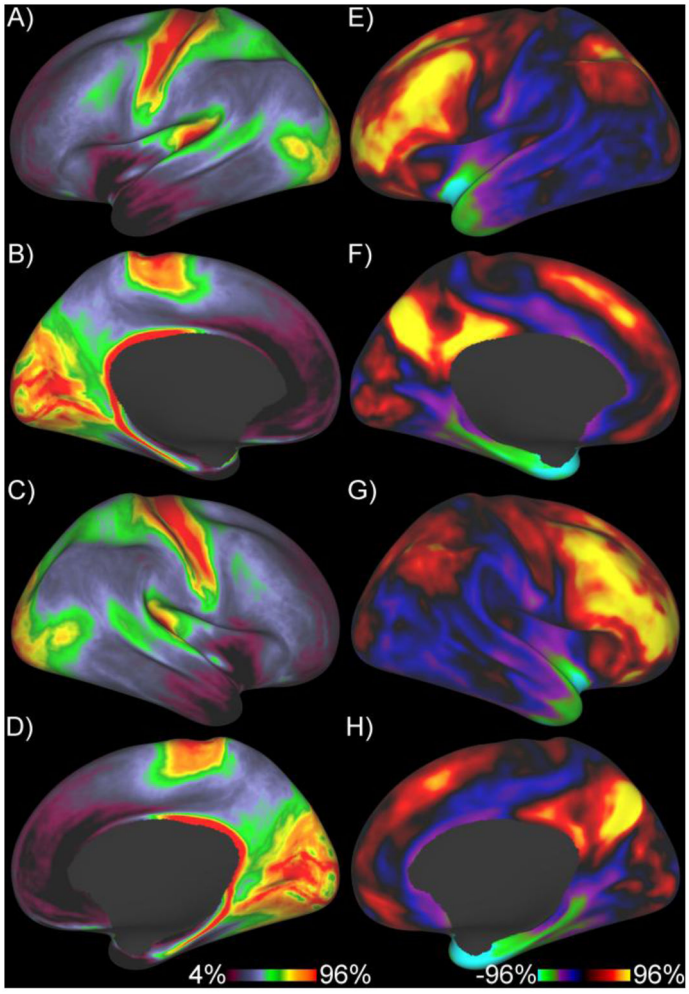

Figure 5.

Myelin maps from Glasser and Van Essen (2011) (A–D) 69-subject MRI data. Partial volume corrected and surface regressed maps of aerobic glycolysis (GI) (E–H) from Vaisnavi et al (2010) 33-subject PET data.

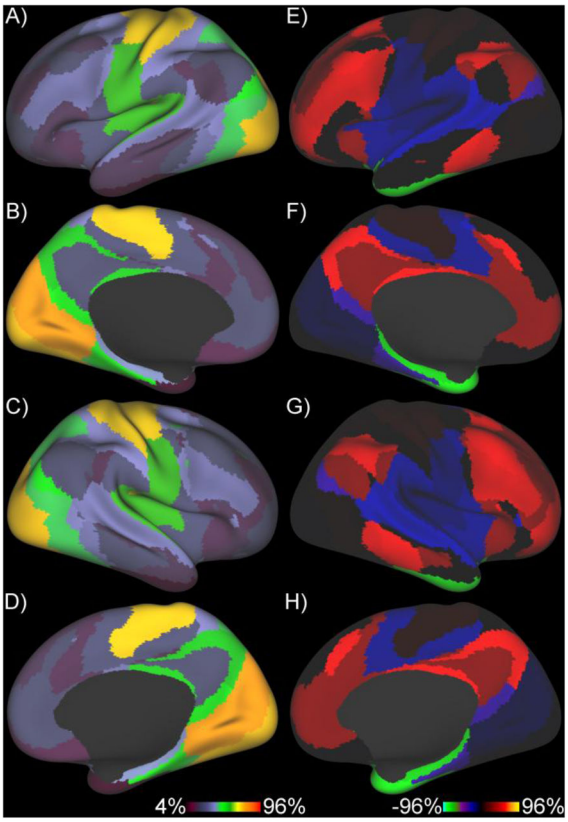

Figure 6.

Mean myelin map (A–D) and aerobic glycolysis (GI) values (E–H) across the Yeo et al 2011 functional network parcellation.